





RESEARCH ARTICLE

The mechanochemical Friedel-Crafts polymerization as a solvent-free cross-linking approach toward microporous polymers

Annika Krusenbaum¹  | Jonathan Geisler¹ | Fabien Joel Leon Kraus¹ |
Sven Grätz¹  | Mark Valentin Höfler² | Torsten Gutmann²  | Lars Borchardt¹ 

¹Inorganic Chemistry I, Ruhr-Universität Bochum, Universitätsstraße 150, Bochum, 44801, Germany

²Technical University Darmstadt, Institute for Inorganic and Physical Chemistry, Alarich-Weiss-Str. 8, Darmstadt, 64287, Germany

Correspondence

Lars Borchardt, Inorganic Chemistry I, Ruhr-Universität Bochum, Universitätsstraße 150, 44801 Bochum, Germany.
Email: lars.borchardt@ruhr-uni-bochum.de

Funding information

TU Darmstadt; Deutsche Forschungsgemeinschaft, Grant/Award Numbers: GU-1650/3-1, 469290370; Bundesministerium für Bildung und Forschung, BMBF, Grant/Award Number: 03SF0498; Federal Ministry of Education and Research

Abstract

Herein we report the mechanochemical Friedel-Crafts alkylation of 1,3,5-triphenylbenzene (TPB) with two organochloride cross-linking agents, dichloromethane (DCM) and chloroform (CHCl₃), respectively. During a thorough milling parameter evaluation, the DCM-linked polymers were found to be flexible and extremely sensitive toward parameter changes, which even enables the synthesis of a polymer with a SSA_{BET} of 1670 m²/g, on par with the solution-based reference. Contrary, CHCl₃-linked polymers are exhibiting a rigid structure, with a high porosity that is widely unaffected by parameter changes. As a result, a polymer with a SSA_{BET} of 1280 m²/g could be generated in as little as 30 minutes, outperforming the reported literature analogue in terms of synthesis time and SSA_{BET}. To underline the environmental benefits of our fast and solvent-free synthesis approach, the green metrics are discussed, revealing an enhancement of the mass intensity, mass productivity and the E-factor, as well as of synthesis time and the work-up in comparison to the classical synthesis. Therefore, the mechanochemical polymerization is presented as a versatile tool, enabling the generation of highly porous polymers within short reaction times, with a minimal use of chlorinated cross-linker and with the possibility of a post polymerization modification.

KEYWORDS

cross-linking, Friedel-Crafts alkylation, high-speed ball milling, mechanochemistry, microporous polymers

1 | INTRODUCTION

The interest in porous materials steadily increased within the last decades, which is attributed to their versatile applicability in several fields of industrial relevance, such as in gas and energy storage, in molecular separation or

in catalysis.^{1–13} While porous materials can be classified regarding their pore sizes as macroporous (pore sizes of >50 nm), as mesoporous (pore sizes of 2–50 nm) or as microporous (pore sizes of <2 nm), the term furthermore includes a variety of different material classes, such as zeolites, carbons or porous metal oxides.^{14–25} Among

This is an open access article under the terms of the Creative Commons Attribution-NonCommercial License, which permits use, distribution and reproduction in any medium, provided the original work is properly cited and is not used for commercial purposes.

© 2021 The Authors. *Journal of Polymer Science* published by Wiley Periodicals LLC.

them, another interesting subcategory are porous polymers, as for instance porous coordination polymers (PCPs), such as metal organic frameworks (MOFs), or porous organic polymers (POPs), which combine the advanced properties of polymers and of porous materials.^{26–33} Especially POPs gain increasing attention, as they are not only characterized by high surface areas and unique pore geometries, but also by a beneficial thermal and chemical stability.^{34–36}

Classically, the syntheses of POPs are accomplished by various solvent-based approaches, which suffer from certain deficiencies.^{37–41} In addition to the issues of rapid precipitation of the products and the need for solubilizing groups, either requiring expensive starting materials or additional synthesis steps, a severe drawback is the generated solvent waste and the accompanied environmental impact.^{42–47}

Solid-state reactions induced by, for example, mechanochemical synthesis procedures, such as high-speed ball milling, overcome these drawbacks and, for this reason, generate growing attention.^{48,49} During a mechanochemical reaction, the collision of the milling balls with the walls of the milling vessel, with the milling material and with themselves results in the transfer of mechanical energy to the involved particles, which initiates a chemical reaction.^{50,51} Recently, Lewis acid catalyzed reactions, such as the Scholl coupling reaction or the Friedel-Crafts alkylation, prevailed for the mechanochemical synthesis of POPs, as they revealed to be both rapid and straightforward and do not require expensive metal catalysts.^{52–59}

Of particular interest in this regard is the origin of porosity, which our group recently investigated exemplified by the mechanochemical Scholl polymerization of 1,3,5-triphenylbenzene (TPB).⁶⁰ Throughout this reaction, the release of HCl was accompanied by a 12 bar pressure increase inside the milling vessel, which was

determined by means of a gas pressure and temperature measurement (GTM) system. This pressure increase was found to directly correlate with the specific surface area of the polymer, considering the ability of the emerging HCl to inflate the polymer. The addition of small quantities of halogenated liquid, the so called liquid-assisted grinding (LAG), was found to further accelerate the reaction by the formation of a highly reactive intermediate and by the volatile nature of the solvent.⁶⁰

In order to obtain a profound knowledge of the pore formation in mechanochemical synthesis procedures, we herein present the Friedel-Crafts alkylation of TPB and DCM or CHCl₃. In contrast to the Scholl reaction, these solvents participate in the reaction as cross-linking agents in equimolar amounts, rather than accelerating the reaction by functioning as liquids for LAG (Figure 1). While the utilization of DCM resulted in the formation of elastic polymers, with a SSA_{BET} highly dependent on the milling parameters, the cross-linking with CHCl₃ was found to yield rigid polymers, seemingly widely unaffected by milling parameter changes. During this study, we examine the role of the amount of cross-linker, the milling time and the milling frequency. Furthermore, we investigate the pore formation by post polymer milling experiments and compare the mechanochemical synthesis approach to the solution based-reference by a detailed green metrics discussion.

2 | RESULTS AND DISCUSSION

2.1 | Mechanochemical Friedel-Crafts alkylation of TPB

The mechanochemical Friedel-Crafts alkylation of TPB was accomplished by the utilization of the two

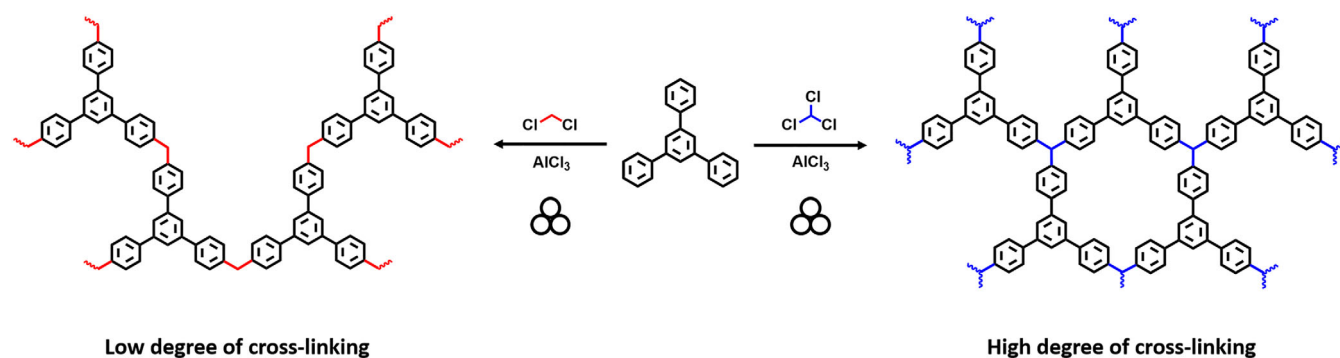


FIGURE 1 Schematic overview over the mechanochemical Friedel-Crafts alkylation of 1,3,5-triphenylbenzene with DCM (left; in red) and with CHCl₃ (right; in blue) as cross-linking agents. In each case, AlCl₃ was utilized as both Lewis acid and bulking material. The polymerization with DCM as cross-linker resulted in the formation of flexible polymers, exhibiting a SSA_{BET} highly dependent on the milling parameters, while the utilization of CHCl₃ generated rigid polymers that were seemingly unaffected by parameter changes

organochloride cross-linking agents DCM and CHCl_3 , respectively. Thereby it was possible to obtain two porous polymers featuring different structural characteristics, since DCM acts as a bidentate cross-linker, while CHCl_3 enables linkage in a tridentate manner (Figure 1). In order to catalyze the reaction, anhydrous AlCl_3 was added to the milling vessel, which additionally served as bulking material. Although the mechanochemical Friedel-Crafts reaction also proceeds with FeCl_3 as catalyst, this approach could potentially result in a competitive oxidative aromatic coupling polymerization as well, which prompted us to employ AlCl_3 as Lewis acid.^{58,59,54,60} During the parameter evaluation special emphasis was put on an environmental benign synthesis approach, therefore water and acetone were chosen to remove excess AlCl_3 , remaining starting materials, or oligomers from the products. In comparison to solution-based approaches, this is a considerable advantage, since MeOH and CHCl_3 are frequently applied for this purpose, although both of them being hazardous for the human operator and the environment.⁴¹ The standardized mechanochemical synthesis approaches, as described in the experimental section, are serving as reference systems herein and will be declared as **FC-DCM-1**

and as **FC- CHCl_3 -1** for the DCM cross-linking synthesis and for the CHCl_3 cross-linking synthesis, respectively. Briefly, the syntheses were performed as follows: 0.5 g (1.63 mmol, 1 eq) TPB and 0.63 ml (9.79 mmol, 6 eq) DCM or 0.78 ml (9.79 mmol, 6 eq) CHCl_3 were milled with 22 ZrO_2 milling balls ($\varnothing = 10$ mm, average weight = 3.14 g) and 5.22 g (39.16 mmol, 24 eq) aluminum(III)chloride for 1 h at 30 Hz and subsequently washed with water and acetone. During the synthesis, a pressure increase of approximately 10 bar (Figure S1) was detected by a GTM system, which was attributed to the HCl released during the reaction.

Both syntheses featured a color change from white-yellow (TPB) to brown, whereas **FC- CHCl_3 -1** exhibited a significantly darker appearance than **FC-DCM-1**. Interestingly, the color change is a first indication that the polymerization is indeed carried out via a Friedel-Crafts alkylation, accomplished by a C1 cross-linking of the organochloride monomer, rather than via a competing oxidative aromatic coupling reaction, that would directly link the TPB monomers with each other. While the oxidative aromatic coupling polymer has a black appearance due to a complete aromatic conjugation, in the given case

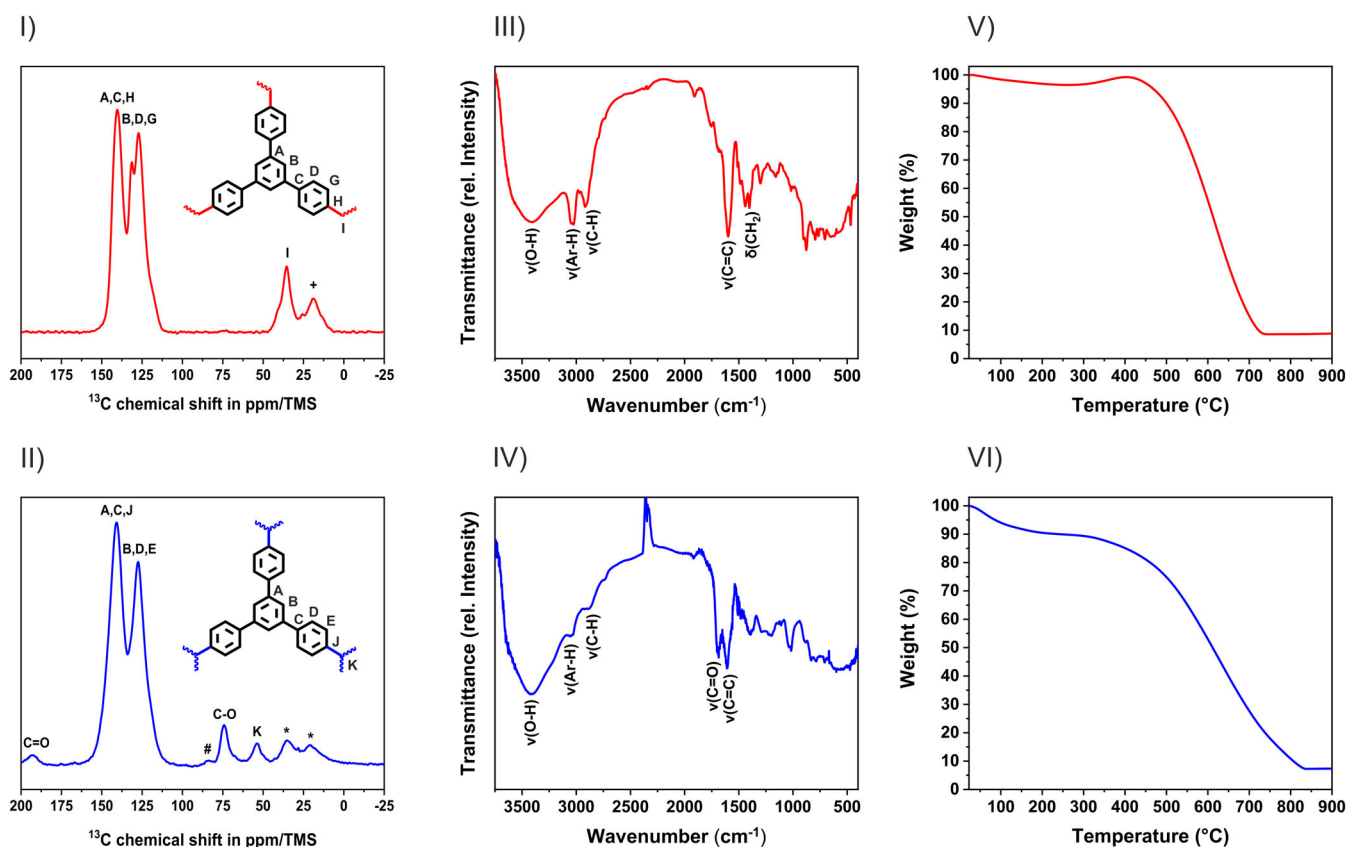


FIGURE 2 (I) & (II) ^{13}C CP MAS spectra of **FC-DCM-1** (I, in red) and **FC- CHCl_3 -1** (II, in blue) measured at 8 kHz and assignment of signals to the carbon atoms of the porous polymers. Spinning sidebands of the aromatic carbon atoms are marked with asterisks, the spinning sideband of $\text{C}=\text{O}$ is marked with a hashtag. (III) & (IV) IR spectra of **FC-DCM-1** (III, in red) and of **FC- CHCl_3** (IV, in blue). (V) & (VI) TGA of **FC-DCM-1** (V, in red) and of **FC- CHCl_3** (VI, in blue)

the cross-linking does not result in an extended aromatic system, as evident by a lighter color of the polymer.⁶⁰

This is additionally verified by the $^1\text{H}\rightarrow^{13}\text{C}$ CP MAS spectra of **FC-DCM-1** and **FC-CHCl₃-1** (Figure 2I,II), as both show two broad signals centered at 127.5 ppm and 140.5 ppm. While the signal at 140.5 ppm is assigned to the quaternary carbon atoms in the materials (A,C,H,J) the signal at 127.5 ppm showing a substructure for **FC-DCM-1** is assigned to carbons in the aromatic ring systems having hydrogen atoms in close vicinity (B,D,E, G). This assignment is underlined by the $^1\text{H}\rightarrow^{13}\text{C}$ FSLG HETCOR experiments (see Figure S2 and Figure S3). The signals at 127.5 ppm and 140.5 ppm show the same chemical shift in the proton dimension. Thereby, the signal at 140.5 ppm has a much lower intensity compared to the signal at 127.5 ppm. Since a short contact time of 200 μs was used for the CP in the $^1\text{H}\rightarrow^{13}\text{C}$ FSLG HETCOR experiments this can be explained by the larger distance of carbon atoms to protons that refer to the signal at 140.5 ppm, and is consistent with the assignment of this signal to quaternary carbons.

For sample **FC-DCM-1** additional signals at 19 ppm and 35.5 ppm with a small shoulder at 41 ppm are visible. The signal at 35.5 ppm can be attributed to the aliphatic CH₂ group of the DCM cross-linker. The signal at 19 ppm marked with a plus maybe assigned an aliphatic CH₃ group, likely generated by mechanochemical degradation of the polymer. Spinning sidebands may mask these peaks but the comparison of the measurements at different spinning frequencies (see Figure S4) show that the spinning sidebands have negligible intensity compared to the isotropic signals in the aliphatic region.

Sample **FC-CHCl₃-1** shows additional signals at 54 ppm, 74 ppm and 192.5 ppm. The signal at 54 ppm can be clearly assigned to the CH group of the tridentate linker. Moreover, due to the hydrolysis of the polymers during the washing procedure a formation of C=O and C—O is possible, which is indicated by the signal at 192.5 ppm and 74 ppm, respectively (see Figure S6).

This is additionally visible in the IR spectrum of **FC-CHCl₃-1** (Figure 2IV), exhibiting a C=O stretching vibration at 1690 cm^{-1} , as well as in the broad bands at approximately 3420 cm^{-1} in both spectra, attributed to an O—H stretching vibration. This O—H stretching vibration is not solely attributed to the C—O—H bonding motif, however it furthermore corresponds to water adsorbed to the samples even after drying in an oven over night. Similar to the solid state ^{13}C -NMR spectra, aliphatic and aromatic bonding motifs are visible for each polymer. While both spectra feature an Ar—H stretching vibration at 3040 cm^{-1} and a C=C stretching vibration at 1600 cm^{-1} , also a C—H stretching vibration is visible at 1755 cm^{-1} . Due to the higher amount of aliphatic C—H

vibrations in the DCM cross-linked polymer, this band is more prominent in the spectrum of **FC-DCM-1** (Figure 2III). Moreover, **FC-DCM-1** features a CH₂ bending vibration at around 1400 cm^{-1} , which derives from the DCM cross-linkage. Both polymers show a high thermal stability of up to 400°C (Figure 2V,VI). The thermogravimetric analysis of **FC-CHCl₃-1** furthermore displays an initial weight loss, which arises from a cleavage of the adsorbed water. This finding is in line with the elemental composition of both polymers by EDS, revealing an oxygen content of 3.31 mass % for **FC-DCM-1** (Table S3) and of 3.61 mass % for **FC-CHCl₃-1** (Table S4). Furthermore, this method allows to monitor the amount of aluminium and chlorine remaining in the polymers after the processing. As both values are below 0.5 mass % for each polymer, the workup is considered as highly sufficient for the removal of excess AlCl₃ and remaining cross-linker. Additionally, zirconium contents of 0.03–0.04 mass % indicate that an abrasion of the milling material is negligible in the given cases. SEM images of the porous polymers reveal flat and layered structures, exhibiting macropores as well as relatively rough surface areas (Figure S9I,II). The layered morphologies are especially visible in the TEM images of both compounds (Figure S9III,IV), which resemble each other, due to the general structural similarity of both polymers.

This is furthermore underlined by the similarity of the specific surface areas of the products. While **FC-DCM-1** features a SSA_{BET} of 1220 m^2/g , the specific surface area of **FC-CHCl₃-1** is slightly higher with 1310 m^2/g . Both polymers feature an IUPAC Type I isotherm with a steep volume uptake in the micropore region (Figure 3I,II). Interestingly, the isotherm of **FC-DCM-1** presents a swelling behavior, which can be attributed to the flexible nature of the bidentate linked polymer. The reason for this is a pore geometry change of the flexible polymer, possibly locking N₂ inside the pores. In contrast, the swelling of **FC-CHCl₃-1** is much less prominent, associated to the rigid tridentate structure. Although both polymers exhibit main pore widths of <2 nm, also smaller mesopores of 2.31–2.53 nm and of 4.15 nm are present (Figure 3III,IV). Analogous to the N₂ physisorption isotherms, both polymers feature a distinct swelling behavior resulting in a hysteresis between adsorption and desorption for CO₂ physisorption measurements. Again, the swelling of **FC-DCM-1** is more prominent than of **FC-CHCl₃-1**, underlining the different flexibilities of both polymers. **FC-CHCl₃-1** and **FC-DCM-1** are capable to store 4.74 mmol CO₂/g and 4.37 mmol CO₂/g, respectively, and are therefore in a comparable range with their solvent-based analogues (4.71 mmol/g (CHCl₃) and 4.35 mmol/g (DCM)) (Figure 3V,VI).⁴¹ Additionally, the CO₂/N₂ selectivity was calculated by

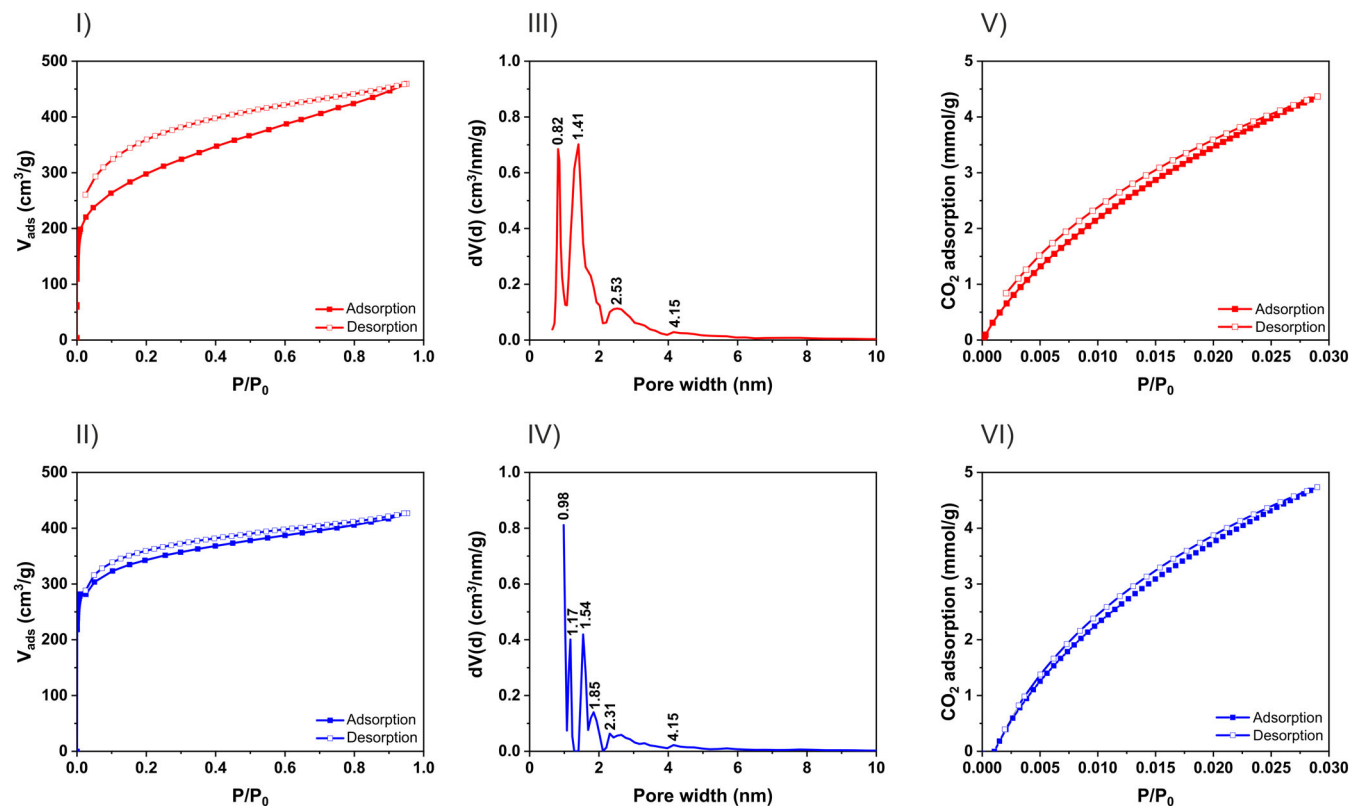


FIGURE 3 Analysis of the porosity of the porous polymers: (I) & (II) N₂ physisorption measurements at 77 K of **FC-DCM-1** (I, in red) and of **FC-CHCl₃-1** (II, in blue). (III) & (IV) Pore size distribution between pores with a width of 0–10 nm of **FC-DCM-1** (III, in red) and of **FC-CHCl₃-1** (IV, in blue). (V) & (VI) CO₂ physisorption measurements of **FC-DCM-1** (V, in red) and of **FC-CHCl₃-1** (VI, in blue) at 273 K between $P/P_0 = 0-0.03$

the ideal adsorption solution theory (IAST) method (for N₂/CO₂) to be 73.98 (90/10) and 93.81 (90/10) for **FC-DCM-1** and **FC-CHCl₃-1**, respectively (Figure S12 and Figure S13).

2.2 | Influence of milling parameters

During the examination of the optimal milling parameters, the amount of cross-linking agent was investigated initially. To rule out the possibility of a competing oxidative aromatic coupling reaction, which would result in the direct linkage of the TPB monomer without the incorporation of a cross-linking agent and therefore in a conjugated polymer, two 0 eq approaches (**FC-DCM-2** and **FC-CHCl₃-2**), with no organochloride liquids added to the milling vessel, were accomplished in proof of principle reactions (see Table S1 and Table S2). As a result, unporous white-yellow powders were obtained, which were readily soluble in water and acetone and were characterized as unreacted TPB (see Figures S14–S17). An explanation for this observation is given by the nature of the Lewis acid AlCl₃. Due to its non-oxidizing character and the inert gas atmosphere inside the milling vessel, the competing oxidative aromatic coupling reaction,

requiring both Lewis acid and oxidant, is inhibited. By the removal of the cross-linking agent, the only possible reaction, the Friedel-Crafts polymerization, is therefore hindered. The addition of 1 eq DCM, however, prompted the formation of a polymer insoluble in water and acetone. Due to the restricted amount of cross-linking agent, the SSA_{BET} and the yield were limited to 50 m²/g and 68%, respectively (Table S1). Accordingly, a further addition of DCM resulted in an enhancement of both SSA_{BET} and yield. It was possible to synthesize a highly porous polymer with a specific surface area of 1670 m²/g by the addition of 15 eq DCM (Figure 4I). This equals an amount of 1.56 ml DCM and is a great improvement in comparison to the solution-based approach. Therein, TPB was stirred in 20 ml DCM for 48 h, which was followed by a work-up including a 24 h Soxhlet extraction in 100 ml MeOH and 100 ml CHCl₃ to yield a polymer with a SSA_{BET} of 1685 m²/g.⁴¹ Our approach is thus capable to not only drastically reduce the amount of cross-linking agent, but to furthermore shorten the synthesis time to 1 h, while the workup is accomplished with water and acetone, yielding a polymer with a similar SSA_{BET}.

While the Friedel-Crafts alkylation utilizing DCM as cross-linker was found to be highly dependent on the amount of utilized cross-linking agent, the CHCl₃ assisted

polymerization was seemingly widely unaffected by equivalent amount changes (Figure 4II). As an example, the addition of 3 eq CHCl_3 already prompted the formation of a porous polymer with a SSA_{BET} of $1230 \text{ m}^2/\text{g}$, while the addition of 15 eq resulted in the formation of a polymer with a specific surface area of $1270 \text{ m}^2/\text{g}$, which are values within a comparable range. An explanation for this might be provided by the structural characteristics of both polymers. In the previous chapter, it was already shown that **FC-DCM-1** is much more flexible than **FC- CHCl_3 -1**. Thus, during synthesis, this polymer has the possibility to rotate and link at different points, while the CHCl_3 cross-linked polymer is more rigid and the synthesis has to follow a fixed blueprint. Therefore, in the DCM assisted syntheses, the equivalent amount of linker not only influences the size of

the network, but it also affects how often the polymer is hyperbranched. The addition of a higher amount of DCM results in a stronger linkage within the polymer, which significantly increases the internal surface area (Table S1).

Evidence for this theory is also provided by the different behavior of both polymers in respect to milling time and frequency changes (Figure 5). As, in general, a goal was to establish a synthesis protocol utilizing as little chlorinated solvent as possible, while obtaining a high and reproducible surface area, milling parameters were evaluated for the polymers synthesized with 6 eq DCM or CHCl_3 , respectively.

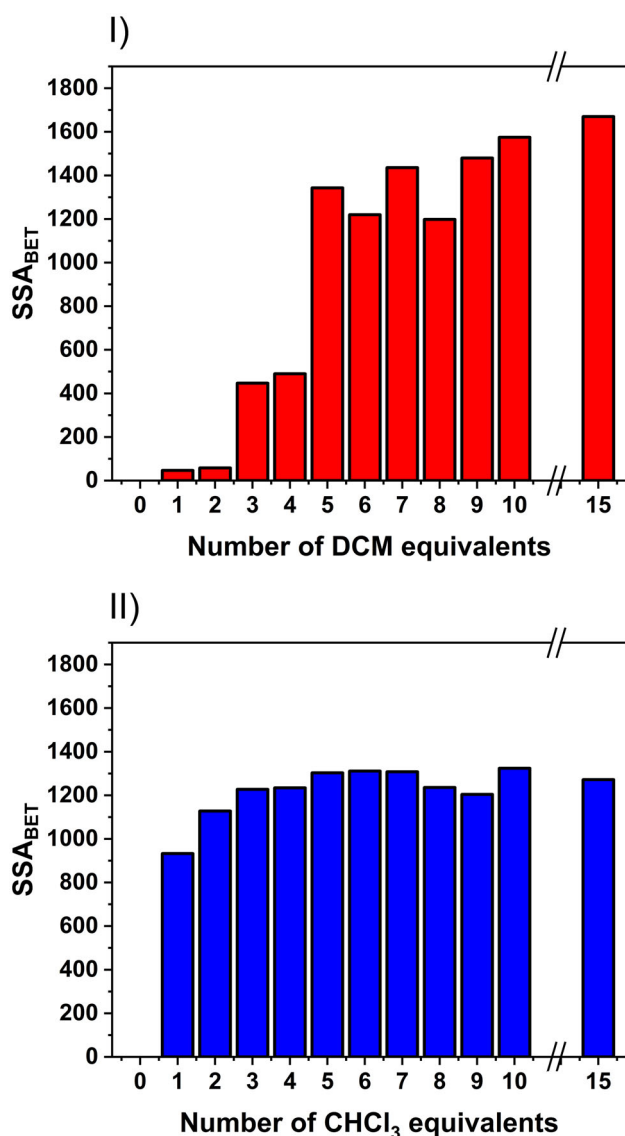


FIGURE 4 SSA_{BET} of porous polymers depending on the number of DCM (I, in red) and CHCl_3 (II, in blue) equivalents utilized for the milling procedure

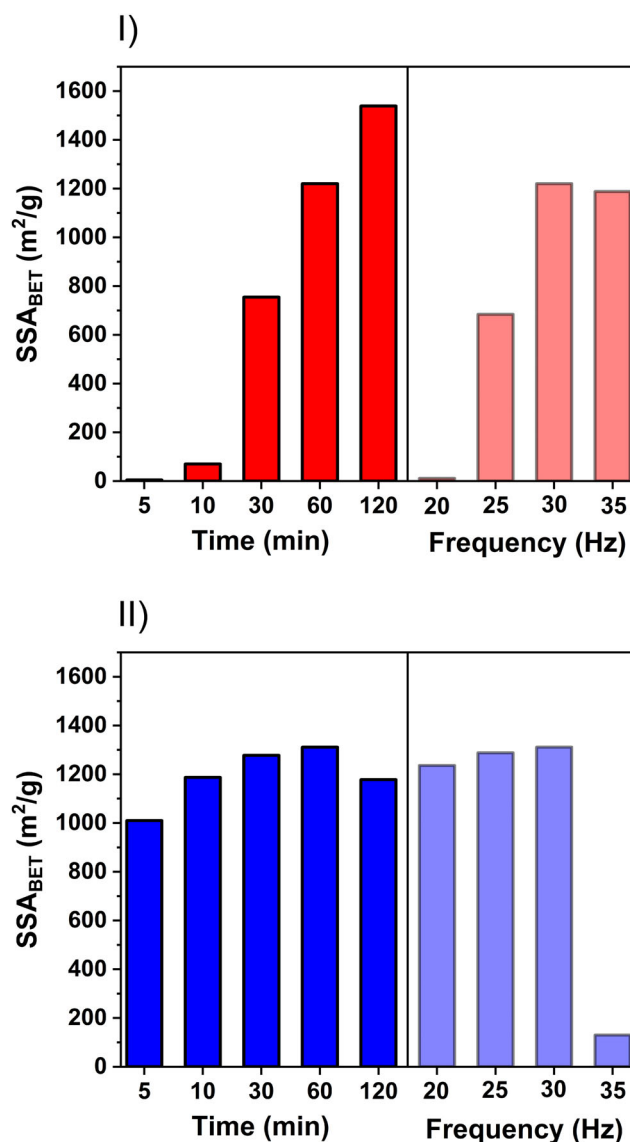


FIGURE 5 SSA_{BET} of porous polymers depending on the milling time (left, dark) and the milling frequency (right; light) for DCM (I, in red) and CHCl_3 (II, in blue) cross-linked polymers. During the milling time evaluation, the frequency was kept at 30 Hz, while the milling frequency evaluation was accomplished within a standard milling time of 60 min. In each case 6 eq of chlorinated cross-linker were utilized

Even though the DCM based synthesis required a synthesis time of at least 60 min for the generation of a sufficiently porous polymer, this goal was already reached after 5 min for the CHCl_3 cross-linking reaction (Figure 5). Likewise, for the FC-DCM polymerization a frequency of 30 Hz was mandatory for a high surface area, while in the analogous CHCl_3 reaction, already 20 Hz were sufficient to achieve this purpose (Figure 5). As a result, the FC-DCM synthesis was found to be highly dependent on the energy-input during the ball milling procedure, which is contrary to the FC- CHCl_3 synthesis. Nevertheless, a further augmentation of the frequency results in a too high energy input, which is capable to destroy the pores of the rigid polymer (Figure 5II). Contrary, the flexible network of the DCM cross-linking synthesis can withstand the high energy input and retain its porosity even at 35 Hz.

To investigate this further, post polymer milling experiments were conducted. Therefore, the as-synthesized polymers **FC-DCM-9** ($1200 \text{ m}^2/\text{g}$) and **FC- CHCl_3 -9** ($1240 \text{ m}^2/\text{g}$) were chosen, as both specific surface areas were found to be in a comparable range. While the milling of the pure polymers, without any bulking AlCl_3 or organochloride cross-linker, led to a drastically reduction of the porosity of both polymers, post polymer milling with the utilization of AlCl_3 only shortly diminished the specific surface areas (see Tables S1 and S2). In a further approach, the polymers were milled with AlCl_3 and 6 eq of the respective organochloride cross-linker. While for **PPM- CHCl_3 -3**, the SSA_{BET} was reduced to $950 \text{ m}^2/\text{g}$, the analogous approach led to a great enhancement of the surface area to $1600 \text{ m}^2/\text{g}$ for **PPM-DCM-3**. This again underlines that the flexible FC-DCM polymers can be modified by adjusting the

synthesis parameters, even after the polymerization is completed, while the rigid CHCl_3 cross-linked polymers break down due to a higher energy input. Nevertheless, this rigidity also results in a certain degree of inertness toward parameter changes for the FC- CHCl_3 polymers with a stable SSA_{BET} , as long as the energy input is not too high.

2.3 | Green metrics discussion

During the parameter evaluation it was possible to generate porous polymers outperforming the solution-based references in terms of SSA_{BET} and yield.⁴¹ Furthermore, the syntheses featured certain environmental benefits, which are traced back to the drastically reduction of chlorinated solvents and an improved work-up. To investigate this further, the solution based approaches were compared to the mechanochemical syntheses regarding several green metrics (Table 1).^{61,62,46,47} A green metrics discussion is based on the 12 principles of green chemistry and enables the standardized quantification of the sustainability of a synthesis. Since various reaction pathways proceed under a variety of different parameters, the evaluation of the sustainability according to several predefined categories is crucial to obtain a comparability of the ecological impact of different reaction processes. For a better comparability, the data were calculated for a reaction of 1 eq TPB with 6 eq cross-linking agent, while the work-up was excluded and will be examined separately. A detailed calculation for each value is presented in the Supporting Information (see Equations S1–S8). The atom economy (AE) for porous polymers generated by a FC cross-linking with DCM is 47.12 for all types of reactions. Nevertheless, the mass intensity (MI) incorporates the total

Reaction	AE	MI	MP	E-factor	<i>t</i>	Work-up
Solvent based DCM ⁴¹	47.12	31.42	3.18	30.34	48 h	^a
MC FC-DCM	47.12	10.56	9.47	8.42	1 h	^b
MC FC-DCM w/o bulk	47.12	4.26	23.47	2.11	1 h	^b
Solvent based CHCl_3 ⁴¹	37.01	36.91	2.71	35.76	48 h	^a
MC FC- CHCl_3	37.01	9.84	10.16	7.46	0.5 h	^b
MC FC- CHCl_3 w/o bulk	37.01	4.26	23.47	1.87	0.5 h	^b

TABLE 1 Comparison of the atom economy (AE), mass intensity (MI), mass productivity (MP), E-factor, synthesis time (*t*) and the work-up for porous polymers synthesized by solvent-based reactions, mechanochemical reactions (MC) and mechanochemical reactions without additional bulk material (MC w/o bulk). The values are compared for the DCM (top) and the CHCl_3 (bottom) cross-linked synthesis, based on a reaction of 6 eq cross-linker and 1 eq TPB. Further information regarding the calculation is available in the Supporting Information (see Equations S1–S8)

^aTwenty-four hours Soxhlet extraction in 100 ml MeOH and 100 ml CHCl_3 ;

^bShort rinse with 100 ml H_2O and 100 ml acetone.

mass of a process, for which reason the solvent-based approach features a high value of 31.42, as 20 ml of DCM are utilized during the synthesis. Since the mechanochemical approach solely requires 0.63 ml of DCM, the MI can be drastically reduced to 10.56 by this method.

As the main process mass of the mechanochemical reaction is attributed to the bulking material AlCl_3 , another calculation was performed for a mechanochemical synthesis without additional bulking agent, suggesting an amount of solely 6 eq AlCl_3 to catalyze the reaction. In this case, the MI can further be lowered to 4.26, which is close to the ideal value of 1 and equals a mass productivity (MP) of 23.47 and an E-factor of 2.11. For the CHCl_3 cross-linking synthesis, a similar observation was accomplished. While the atom economy is slightly lower for all processes in comparison to the DCM synthesis, which is due to the additional chlorine atom of CHCl_3 that is cleaved during the reaction, the mass productivity of a mechanochemical approach without bulking material is nearly one order of magnitude higher than for the solution-based approach. In addition to the drastically enhancement of both syntheses protocols by the utilization of a mechanochemical method, the sustainability of the work-up was increased enormous, since the 24 h Soxhlet extraction in a mixture of 100 ml MeOH and 100 ml CHCl_3 could be substituted by a short rinse of the products with water and acetone. Likewise, the general synthesis time could be shortened drastically from 48 h for both solution-based approaches to 1 h (FC-DCM). For the synthesis of the CHCl_3 cross-linked polymer it was even possible to generate a porous polymer with a SSA_{BET} of $1280 \text{ m}^2/\text{g}$ within 30 min, which is outperforming the solution-based approach in terms of yield and specific surface area.⁴¹

3 | CONCLUSION

Herein we reported the mechanochemical synthesis of microporous polymers by a Friedel-Crafts reaction, utilizing different organochloride solvents as cross-linking agents. While the solvents were found to play a tremendous role for the reaction, ruling out a competing oxidative aromatic coupling reaction, the careful parameter evaluation provided a significant insight into the polymer characteristics and the pore formation. While the DCM-based syntheses resulted in the formation of flexible polymers, highly dependent on the utilized parameters, the CHCl_3 cross-linking promoted the generation of rigid polymers, widely unaffected by parameter changes. Therefore, it was possible to synthesize a porous polymer within 30 min, outperforming the solution-based analogue in terms of SSA_{BET} , yield, synthesis time and sustainability. For a further investigation a detailed green metrics discussion was performed, revealing an enormous enhancement of the

sustainability of a Friedel-Crafts reaction by the application of a mechanochemical synthesis approach.

4 | EXPERIMENTAL SECTION

4.1 | Mechanochemical Friedel-Crafts polymerization

For the synthesis of a dichloromethane cross-linked polymer, 0.5 g (1.63 mmol, 1 eq) 1,3,5-triphenylbenzene, 0.63 ml (9.79 mmol, 6 eq) predried dichloromethane and 5.22 g (39.16 mmol, 24 eq) aluminium(III)chloride, acting both as bulk material and as Lewis acid, were placed in a 50 ml ZrO_2 milling vessel under inert gas atmosphere. Twenty-two ZrO_2 milling balls ($\text{Ø} = 10 \text{ mm}$, average weight = 3.14 g) were added and the mixture was milled for 1 h at 30 Hz in a Retsch mixer mill MM500. Afterwards, the crude product was subsequently washed with water and acetone and was dried at 80°C over night.

Physical data: $^1\text{H} \rightarrow ^{13}\text{C}$ CP MAS (300 MHz/75 MHz, δ): 140.5 (—C=), 127.5 (HC=), 35.5 (CH_2); IR (KBr): $\nu = 3420 \text{ cm}^{-1}$ (w; $\nu[\text{O—H}]$), 3040 cm^{-1} (w; $\nu[\text{Ar—H}]$), 1755 cm^{-1} (w; $\nu[\text{C—H}]$), 1600 cm^{-1} (m; $\nu[\text{C=C}]$), 1400 cm^{-1} (w; $\delta(\text{CH}_2)$).

To synthesize the chloroform cross-linked polymer 0.78 ml (9.79 mmol, 6 eq) predried chloroform were added to the milling jar occupied with 0.5 g (1.63 mmol, 1 eq) 1,3,5-triphenylbenzene and 5.22 g (39.16 mmol, 24 eq) aluminium(III)chloride under inert-gas atmosphere. Afterwards, the milling and washing procedure was accomplished in an analogous fashion to aforementioned.

Physical data: $^1\text{H} \rightarrow ^{13}\text{C}$ CP MAS (300 MHz/75 MHz, δ): 192.5 (C=O), 140.5 (—C=), 127.5 (HC=), 74 (C—O), 54 (CH); IR (KBr): $\nu = 3420 \text{ cm}^{-1}$ (w; $\nu[\text{O—H}]$), 3040 cm^{-1} (w; $\nu[\text{Ar—H}]$), 1755 cm^{-1} (w; $\nu[\text{C—H}]$), 1690 cm^{-1} (s; $\nu(\text{C=O})$), 1600 cm^{-1} (m; $\nu[\text{C=C}]$).

4.2 | Analysis

4.2.1 | Solid state NMR

All measurements were performed at 7 T on a Bruker Avance III HD 300 spectrometer. This system is equipped with a 4 mm $^1\text{H}/\text{X}$ probe operating at 300.11 MHz for ^1H and 75.47 MHz for ^{13}C . $^1\text{H} \rightarrow ^{13}\text{C}$ CP MAS experiments were performed employing a ramp on ^1H during contact. The contact time was set to 3 ms and the recycle delay was set to 1 s. The acquisition time was 24 ms and TPPM decoupling⁶³ was applied during data acquisition. The spinning frequency was set to 8 kHz, 5 kHz and 6 kHz, respectively, and 10,240 scans were applied to record each

spectrum. The spectra were referenced to TMS (0 ppm) using adamantane (38.5 ppm) as an external standard. The $^1\text{H} \rightarrow ^{13}\text{C}$ CP MAS spectrum of the reference sample **FC-DCM-2** was recorded similarly, employing a recycle delay of 18 s and 256 scans. The $^1\text{H} \rightarrow ^{13}\text{C}$ FSLG HETCOR experiments were performed with a contact time 200 μs and a ramp on ^1H during contact. During evolution of the ^1H chemical shift homonuclear Frequency Switched Lee Goldberg decoupling⁶⁴ was applied with a field strength of 72 kHz. Sixty-four slices were recorded with 922 scans per slice. The acquisition time was set to 35 ms and TPPM heteronuclear decoupling⁶³ was applied during data acquisition. The ^{13}C dimension was referenced to TMS (0 ppm) using adamantane (38.5 ppm, 1.78 ppm) as an external standard. The ^1H dimension was referenced to the aromatic signal at 6.3 ppm.

4.2.2 | IR

Infrared spectroscopy was carried out on a SHIMADZU IRSpirit Fourier transform infrared spectrometer equipped with a diffuse reflectance device. The spectra were recorded with 45 scans between 400 cm^{-1} and 3750 cm^{-1} . Prior to the measurement, a spatula tip of the respective sample was mixed with approximately 10 mg of KBr.

4.2.3 | TGA

Thermogravimetric analysis was performed on a Pyris 6 device from Perkin Elmer. Therefore, 3 mg of the respective sample were filled into aluminium crucibles and were heated to 900°C degree with a heating rate of 10°C per minute.

4.2.4 | TEM/STEM/EDS

TEM and STEM images were recorded on a JEOL, JEM-2800 instrument with a high resolution of 90 pm (TEM) and of 160 pm (STEM), respectively. Additionally, the samples were analyzed by a dual SSD-EDS-System (resolution: 1 nm). Therefore, all samples were suspended in EtOH and applied to a grid consisting of Lacey Carbon Films on 400 Mesh Copper.

4.2.5 | Physisorption measurements


The porosity of all synthesized polymers was determined by physisorption measurements on a Quantachrome Quadrasorb instrument at 77 K. Prior to the measurements, all samples were outgassed under vacuum for 24 h at 423 K.

During the measurements, high purity nitrogen gas (N_2 : 99.999%) was used. The determination of specific surface areas (SSA) was accomplished with the help of the BET (Brunauer, Emmett, Teller) equation, while pore size distributions were calculated by the DFT (Density Functional Theory) method for slit, cylindrical and sphere pores and total pore volumes were estimated at the adsorption branch at $P/P_0 = 0.95$. In addition, CO_2 adsorption measurements were performed on an Quantachrome Autosorb instrument at 273 K and at 298 K. Therefore, the samples were outgassed in a similar fashion to aforementioned.

ACKNOWLEDGMENTS

L.B., S.G., and A.K. gratefully acknowledge the Federal Ministry of Education and Research (Bundesministerium für Bildung und Forschung, BMBF) for support of the Mechanocarb project (award number 03SF0498) and the Deutsche Forschungsgemeinschaft for funding the Project 469290370. T.G. thanks the DFG under contract GU-1650/3-1 for financial support. We thank Prof. Buntkowsky (TU Darmstadt) for generous allocation of measurement time at his Bruker Avance III HD 300 NMR spectrometer.

ORCID

Annika Krusenbaum  <https://orcid.org/0000-0002-2848-3652>

Sven Grätz  <https://orcid.org/0000-0001-6026-097X>

Torsten Gutmann  <https://orcid.org/0000-0001-6214-2272>

Lars Borchardt  <https://orcid.org/0000-0002-8778-7816>

REFERENCES

- [1] P. Kaur, J. T. Hupp, S. T. Nguyen, *ACS Catal.* **2011**, *1*, 819.
- [2] S. Kitagawa, R. Kitaura, S. Noro, *Angew. Chem., Int. Ed.* **2004**, *43*, 2334.
- [3] an Li, R.-F. Lu, Y. Wang, X. Wang, K.-L. Han, W.-Q. Deng, *Angew. Chem., Int. Ed.* **2010**, *49*, 3330.
- [4] K. Cousins, R. Zhang, *Polymer* **2019**, *11*, 690.
- [5] W. Lu, D. Yuan, D. Zhao, C. I. Schilling, O. Plietzsch, T. Muller, S. Bräse, J. Guenther, J. Blümel, R. Krishna, Z. Li, H.-C. Zhou, *Chem. Mater.* **2010**, *22*, 5964.
- [6] W. Li, J. Liu, D. Zhao, *Nat. Rev. Mater.* **2016**, *1*, 16023.
- [7] L. Wang, J. Ding, S. Sun, B. Zhang, X. Tian, J. Zhu, S. Song, B. Liu, X. Zhuang, Y. Chen, *Adv. Mater. Interfaces* **2018**, *5*, 1701679.
- [8] O. M. Yaghi, H. Li, C. Davis, D. Richardson, T. L. Groy, *Acc. Chem. Res.* **1998**, *31*, 474.
- [9] J.-X. Jiang, F. Su, A. Trewin, C. D. Wood, N. L. Campbell, H. Niu, C. Dickinson, A. Y. Ganin, M. J. Rosseinsky, Y. Z. Khimiyak, A. I. Cooper, *Angew. Chem., Int. Ed.* **2007**, *46*, 8574.
- [10] N. B. McKeown, P. M. Budd, *Chem. Soc. Rev.* **2006**, *35*, 675.
- [11] Q. Sun, Z. Dai, X. Meng, F.-S. Xiao, *Chem. Soc. Rev.* **2015**, *44*, 6018.
- [12] S. Kim, B. Kim, N. A. Dogan, C. T. Yavuz, *ACS Sustainable Chem. Eng.* **2019**, *7*, 10865.
- [13] K. Dong, Q. Sun, X. Meng, F.-S. Xiao, *Catal. Sci. Technol.* **2017**, *7*, 1028.

- [14] K. Ariga, A. Vinu, Y. Yamauchi, Q. Ji, J. P. Hill, *Bull. Chem. Soc. Jpn.* **2012**, 85, 1.
- [15] D. Xu, J. Guo, F. Yan, *Prog. Polym. Sci.* **2018**, 79, 121.
- [16] M. M. Zagho, M. K. Hassan, M. Khraisheh, M. A. A. Al-Maadeed, S. Nazarenko, *Chem. Eng. J. Adv.* **2021**, 6, 100091.
- [17] S. Li, J. Li, M. Dong, S. Fan, T. Zhao, J. Wang, W. Fan, *Chem. Soc. Rev.* **2019**, 48, 885.
- [18] P. Zhu, S. Meier, S. Saravanamurugan, A. Riisager, *Mol. Catal.* **2021**, 510, 111686.
- [19] M. E. Casco, F. Badaczewski, S. Grätz, A. Tolosa, V. Presser, B. M. Smarsly, L. Borchardt, *Carbon* **2018**, 139, 325.
- [20] M. E. Casco, E. Zhang, S. Grätz, S. Krause, V. Bon, D. Wallacher, N. Grimm, D. M. Többens, T. Hauß, L. Borchardt, *J. Phys. Chem. C* **2019**, 123, 24071.
- [21] D. Leistenschneider, N. Jäckel, F. Hippauf, V. Presser, L. Borchardt, *Beilstein J. Org. Chem.* **2017**, 13, 1332.
- [22] D. Leistenschneider, K. Wegner, C. Eßbach, M. Sander, C. Schneidermann, L. Borchardt, *Carbon* **2019**, 147, 43.
- [23] C. Schneidermann, C. Kensy, P. Otto, S. Oswald, L. Giebeler, D. Leistenschneider, S. Grätz, S. Dörfler, S. Kaskel, L. Borchardt, *ChemSusChem* **2019**, 12, 310.
- [24] W. Xiao, S. Yang, P. Zhang, P. Li, P. Wu, M. Li, N. Chen, K. Jie, C. Huang, N. Zhang, S. Dai, *Chem. Mater.* **2018**, 30, 2924.
- [25] A. Huang, Y. He, Y. Zhou, Y. Zhou, Y. Yang, J. Zhang, L. Luo, Q. Mao, D. Hou, J. Yang, *J. Mater. Sci.* **2019**, 54, 949.
- [26] J.-S. M. Lee, K. Otake, S. Kitagawa, *Coord. Chem. Rev.* **2020**, 421, 213447.
- [27] S. Noro, J. Mizutani, Y. Hijikata, R. Matsuda, H. Sato, S. Kitagawa, K. Sugimoto, Y. Inubushi, K. Kubo, T. Nakamura, *Nat. Commun.* **2015**, 6, 5851.
- [28] A. M. P. Peedikakkal, N. N. Adarsh, in *Polymers and Polymeric Composites: A Reference Series* (Ed: M. I. H. Mondal), Springer International Publishing; Imprint: Springer, Cham **2020**, p. 1.
- [29] C.-A. Tao, J.-F. Wang, *Crystals* **2021**, 11, 15.
- [30] T. Friščić, in *Encyclopedia of inorganic and bioinorganic chemistry* (Ed: R. A. Scott), John Wiley and Sons, Inc, Hoboken, NJ **2011**, p. 1.
- [31] M. E. Casco, F. Rey, J. L. Jordá, S. Rudić, F. Fauth, M. Martínez-Escandell, F. Rodríguez-Reinoso, E. V. Ramos-Fernández, J. Silvestre-Albero, *Chem. Sci.* **2016**, 7, 3658.
- [32] T.-X. Wang, H.-P. Liang, D. A. Anito, X. Ding, B.-H. Han, *J. Mater. Chem. A* **2020**, 8, 7003.
- [33] T. Zhang, G. Xing, W. Chen, L. Chen, *Mater. Chem. Front.* **2020**, 4, 332.
- [34] H. L. Nguyen, N. Hanikel, S. J. Lyle, C. Zhu, D. M. Proserpio, O. M. Yaghi, *J. Am. Chem. Soc.* **2020**, 142, 2218.
- [35] X. Xie, J. Wang, J. Zheng, J. Huang, C. Ni, J. Cheng, Z. Hao, G. Ouyang, *Anal. Chim. Acta* **2018**, 1029, 30.
- [36] F. M. Wisser, K. Eckhardt, D. Wisser, W. Böhlmann, J. Grothe, E. Brunner, S. Kaskel, *Macromolecules* **2014**, 47, 4210.
- [37] P. Pandey, O. K. Farha, A. M. Spokoyny, C. A. Mirkin, M. G. Kanatzidis, J. T. Hupp, S. T. Nguyen, *J. Mater. Chem.* **2011**, 21, 1700.
- [38] Z. Guo, P. Sun, X. Zhang, J. Lin, T. Shi, S. Liu, A. Sun, Z. Li, *Chem. – Asian J.* **2018**, 13, 2046.
- [39] L. Pan, Q. Chen, J.-H. Zhu, J.-G. Yu, Y.-J. He, B.-H. Han, *Polym. Chem.* **2015**, 6, 2478.
- [40] J. Schmidt, J. Weber, J. D. Epping, M. Antonietti, A. Thomas, *Adv. Mater.* **2009**, 21, 702.
- [41] V. Rozyyev, Y. Hong, M. S. Yavuz, D. Thirion, C. T. Yavuz, *Adv. Energy Sustainability Res.* **2021**, 2(10), 2100064.
- [42] X.-J. Zhang, N. Bian, L.-J. Mao, Q. Chen, L. Fang, A.-D. Qi, B.-H. Han, *Macromol. Chem. Phys.* **2012**, 213, 1575.
- [43] M.-Y. Wang, Q.-J. Zhang, Q.-Q. Shen, Q.-Y. Li, S.-J. Ren, *Chin. J. Polym. Sci.* **2020**, 38, 151.
- [44] R. A. Sheldon, *ACS Sustainable Chem. Eng.* **2018**, 6, 32.
- [45] P. Anastas, N. Eghbali, *Chem. Soc. Rev.* **2010**, 39, 301.
- [46] H. C. Erythropel, J. B. Zimmerman, T. M. de Winter, L. Petitjean, F. Melnikov, C. H. Lam, A. W. Lounsbury, K. E. Mellor, N. Z. Janković, Q. Tu, L. N. Pincus, M. M. Falinski, W. Shi, P. Coish, D. L. Plata, P. T. Anastas, *Green Chem.* **2018**, 20, 1929.
- [47] M. Tobiszewski, M. Marć, A. Gałuszka, J. Namieśnik, *Molecules* **2015**, 20, 10928.
- [48] A. Stolle, T. Szuppa, S. E. S. Leonhardt, B. Ondruschka, *Chem. Soc. Rev.* **2011**, 40, 2317.
- [49] S. Grätz, B. Wolfrum, L. Borchardt, *Green Chem.* **2017**, 19, 2973.
- [50] J. L. Howard, Q. Cao, D. L. Browne, *Chem. Sci.* **2018**, 9, 3080.
- [51] C. Bolm, J. G. Hernández, *Angew. Chem., Int. Ed.* **2019**, 58, 3285.
- [52] X. Zhu, C. Tian, T. Jin, K. L. Browning, R. L. Sacci, G. M. Veith, S. Dai, *ACS Macro Lett.* **2017**, 6, 1056.
- [53] R. Yuan, Z. Yan, A. Shaga, H. He, *J. Solid State Chem.* **2020**, 287, 121327.
- [54] S. Grätz, M. Oltermann, E. Troschke, S. Paasch, S. Krause, E. Brunner, L. Borchardt, *J. Mater. Chem. A* **2018**, 6, 21901.
- [55] X. Zhu, Y. Hua, C. Tian, C. W. Abney, P. Zhang, T. Jin, G. Liu, K. L. Browning, R. L. Sacci, G. M. Veith, H.-C. Zhou, W. Jin, S. Dai, *Angew. Chem., Int. Ed.* **2018**, 57, 2816.
- [56] E. Troschke, S. Grätz, T. Lübken, L. Borchardt, *Angew. Chem., Int. Ed.* **2017**, 56, 6859.
- [57] Q. Pan, Z. Xu, S. Deng, F. Zhang, H. Li, Y. Cheng, L. Wei, J. Wang, B. Zhou, *RSC Adv.* **2019**, 9, 39332.
- [58] S. Grätz, S. Zink, H. Krafczyk, M. Rose, L. Borchardt, *Beilstein J. Org. Chem.* **2019**, 15, 1154.
- [59] J.-S. M. Lee, T. Kurihara, S. Horike, *Chem. Mater.* **2020**, 32, 7694.
- [60] A. Krusenbaum, S. Grätz, S. Bimmermann, S. Hutsch, L. Borchardt, *RSC Adv.* **2020**, 10, 25509.
- [61] D. J. C. Constable, A. D. Curzons, V. L. Cunningham, *Green Chem.* **2002**, 4, 521.
- [62] A. D. Curzons, D. N. Mortimer, D. J. C. Constable, V. L. Cunningham, *Green Chem.* **2001**, 3, 1.
- [63] A. E. Bennett, C. M. Rienstra, M. Auger, K. V. Lakshmi, R. G. Griffin, *J. Chem. Phys.* **1995**, 103, 6951.
- [64] B.-J. van Rossum, H. Förster, H. de Groot, *J. Magn. Reson.* **1997**, 124, 516.

SUPPORTING INFORMATION

Additional supporting information may be found in the online version of the article at the publisher's website.

How to cite this article: A. Krusenbaum, J. Geisler, F. J. L. Kraus, S. Grätz, M. V. Höfler, T. Gutmann, L. Borchardt, *J. Polym. Sci.* **2022**, 60(1), 62. <https://doi.org/10.1002/pol.20210606>